Biosensors and Bioelectronics 130 (2019) 389–396

Contents lists available at ScienceDirect

Biosensors and Bioelectronics

journal homepage: www.elsevier.com/locate/bios

A folding affinity paper-based electrochemical impedance device for cardiovascular risk assessment

Yuwadee Boonyasit[a], Orawon Chailapakul[b,c], Wanida Laiwattanapaisal[a,c,*]

[a] Department of Clinical Chemistry, Faculty of Allied Health Sciences, Chulalongkorn University, Bangkok 10330, Thailand
[b] Department of Chemistry, Faculty of Science, Chulalongkorn University, Bangkok 10330, Thailand
[c] Electrochemistry and Optical Spectroscopy Center of Excellence (EOSCE), Chulalongkorn University, Bangkok 10330, Thailand

ARTICLE INFO

Keywords:
C-reactive protein
Cardiovascular risk assessment
Paper-based electrochemical impedance device
Phosphocholine-based detection
Label-free electrochemical detection
Single frequency analysis

ABSTRACT

A novel affinity paper-based electrochemical impedance device (PEID) was first fully developed for cardiovascular risk assessment. Herein, a simple folding PEID comprising a dual screen-printed electrode was fabricated for label-free electrochemical impedance detection. The results demonstrated in a step-wise manner that the phosphocholine-modified screen-printed carbon electrodes were highly responsive to the clinically required range of C-reactive protein (CRP) (0.005 – 500 mg L^{-1}; r^2 = 0.993) levels with a detection limit (3σ/slope) of 0.001 mg L^{-1}. The optimal binding frequency of CRP–phosphocholine interaction was determined to be 100 Hz. These results implied that our proposed system could be used for simultaneously measuring the CRP levels using a single PEID platform in combination with the specific recognition elements. When assaying two levels of CRP, the overall assay reproducibility for each concentration, expressed as relative standard error of the mean (RSE%; n = 30), was 1.21%. The variation in the measurements between individual electrodes, expressed as the relative standard deviation (RSD), was 2.82%. Using 2 measurement sites per device, the proposed sensor provided excellent precision for the simultaneous detection of CRP. Moreover, the RSD for the CRP levels measured on ten independently fabricated paper-based sheets was 2.11%, thereby offering an acceptable fabrication reproducibility. The presented folding PEIDs were used forthe determination of CRP in patient-derived blood samples with minimised bias and excellent correlation with a standard method (n = 15; CUSUM linearity test, p > 0.10), thus permitting the potential application of PEID for assessing cardiovascular risk in individuals.

1. Introduction

Typically, the measurement of biomarkers for the early detection of cardiovascular disease in asymptomatic individuals is vitally important because the prevention of disease is better than the treatment. Thus, the development of methods for detecting the markers of cardiovascular risk assessment is absolutely crucial. Currently, although the determination of plasma lipid profiles, i.e. total cholesterol, triglycerides, and high density lipoprotein cholesterol (HDL), is considered a useful prognostic indicator of risk assessment for atherosclerosis, the picture provided by lipid profiles alone is still incomplete for assessing the risk of future coronary events in healthy individuals (Libby and Ridker, 2004). Recently, emerging evidence has suggested that the measurement of inflammatory markers, particularly serum or plasma C-reactive protein (CRP), improves the prediction of coronary risk evaluation (Libby and Ridker, 2004; Ridker, 2003). CRP can predict the risk of future coronary events in individuals without any prior evidence of cardiovascular disease (Park et al., 2012). The elevated serum or plasma CRP has been associated with increased future risk of acute myocardial infarction (AMI) and thus helps with the implementation of timely therapeutic interventions (Rifai and Ridker, 2001).

CRP, an acute phase protein, has attracted considerable attention as a biomarker for global cardiovascular disease risk prediction and plays a prominent role in the pathogenesis of atherosclerosis, which contributes to myocardial infarction. The American Heart Association and the United States Centre for Disease Control have classified the CRP concentrations for evaluating the cardiovascular disease risk as follows: a CRP concentration below 1.0 mg L^{-1} represents a low risk, the 1.0 – 3.0 mg L^{-1} range an average risk, and levels above 3.0 mg L^{-1} represent a high risk (Roberts, 2004). Reliable methods for the quantification of CRP concentration have therefore become important for improving the outcome of cardiovascular disease through appropriate interventions or treatment.

Current methods to detect CRP levels depend heavily on antibody-

* Corresponding author at: Department of Clinical Chemistry, Faculty of Allied Health Sciences, Chulalongkorn University, Bangkok 10330, Thailand.
E-mail address: Wanida.L@chula.ac.th (W. Laiwattanapaisal).

https://doi.org/10.1016/j.bios.2018.09.031
Received 30 June 2018; Received in revised form 1 September 2018; Accepted 8 September 2018
Available online 12 September 2018
0956-5663/

based assays such as immunoturbidimetry (Borque et al., 2000; Dupuy et al., 2003), immunoagglutination (Senju et al., 1986; Thomas and Coakley, 1996), and the enzyme-linked immunosorbent assay (ELISA) (Sadir et al., 2014; Wu et al., 2007), most of which rely on a wide range of techniques, including optical methods (e.g., colorimetric detection (Christodoulides et al., 2002; Vashist et al., 2014; Zhou et al., 2012), chemiluminescence (Bhattacharyya and Klapperich, 2007), fluorescence (Ahn et al., 2003; Islam et al., 2010; Oh et al., 2005; Peoples and Karnes, 2008; Phurimsak et al., 2016, 2014), surface plasmon resonance (Hu et al., 2006; Meyer et al., 2006), metal clad leaky waveguide (Kim et al., 2014), white light reflectance spectroscopy (Koukouvinos et al., 2016), and surface enhanced Raman spectroscopy (Noble et al., 2012)), electrochemical methods (e.g., amperometric techniques (de Ávila et al., 2013; Kazimierczak et al., 2016), voltammetric techniques (Kokkinos et al., 2015; Zhou et al., 2010), electrochemical impedance spectroscopy (EIS) (Bryan et al., 2013; Fernandes et al., 2014; Hennessey et al., 2009; Lehr et al., 2014; Park et al., 2008; Prasad et al., 2013; Singal and Kotnala, 2017; Vattipalli et al., 2010; Vermeeren et al., 2011), and electrogenerated chemiluminescence (Ala-Kleme et al., 2006; Miao and Bard, 2003; O'Reilly et al., 2015)), mass spectrometry (Kiernan et al., 2006; Meyer and Ueland, 2014), magnetic permeability detection (Kriz et al., 2005; Meyer et al., 2007), piezoelectric sensors (Gan et al., 2012, 2013), surface acoustic wave-based sensors (McBride and Cooper, 2008; Mitsakakis and Gizeli, 2011), and field effect transistor-based sensors (Kim et al., 2013a). The other techniques for CRP determination are based either on biological or chemical recognition elements such as DNA hybridisation (Songjaroen et al., 2016), DNA or RNA aptamers (Centi et al., 2009; Pultar et al., 2009; Yang et al., 2009)], phosphocholine residues (Deegan et al., 2003; Goda et al., 2015; Kim et al., 2011; Kitayama and Takeuchi, 2014; Pomowski et al., 2015), phosphorylethanolamine (Raj et al., 2007), and molecular imprinting polymers (Kumar and Prasad, 2012). However, most of the aforementioned approaches require sophisticated instrumentation with multiple operation steps. Moreover, some techniques lack the desired sensitivity to determine the concentration of CRP in apparently healthy persons. Consequently, the further development of methods for determining the high-sensitivity CRP (hs-CRP) is needed.

EIS-based platforms provide great potential for developing label-free ultrasensitive diagnostic sensors for determining protein biomarkers such as diabetic markers (Boonyasit et al., 2016a, 2015, 2016b), inflammatory markers (Fairchild et al., 2009; La Belle et al., 2011), cancer markers (Elshafey et al., 2013), and cardiac markers (Periyakaruppan et al., 2013). EIS provides a clear understanding of the signal transduction processes occurring at the electrode interface, reflecting the physical and chemical structure in the amplitude and phase of the response (Lasseter et al., 2004). More recently, a single frequency impedance analysis has attracted great interest in biosensing applications since the measurement of impedance over a wide frequency range is relatively time consuming (Katz et al., 2001; Shervedani and Hatefi-Mehrjardi, 2007; Shervedani and Mozaffari, 2006). A unique frequency upon binding occurs when the target molecule binds specifically to its recognition element. Although a single frequency analysis was previously achieved on antibody-based sensors for CRP determination, the analytical characteristics, i.e., sensitivity, selectivity, reproducibility, and storage stability, need to be improved to meet the clinical requirements (Singal and Kotnala, 2017).

Herein, a folding affinity paper-based electrochemical impedance device (PEID) was developed for the ultrasensitive label-free EIS detection of CRP over the clinically relevant concentration range. The folding technique can be integrated with the fabrication of PEID, which provides a one-step method for patterning paper-based devices. Interestingly, a simple folding step aimed to create a small chamber for the electrochemical cell buffer. The proposed PEID has been implemented for hs-CRP determination based solely on the calcium-dependent binding affinity of CRP for phosphocholine. The binding interaction between CRP and the phosphocholine-based recognition was also investigated for the specific optimal binding frequency upon binding. To the best of our knowledge, the presented PEID system is the first one capable of assessing CRP levels in real clinical blood samples. Moreover, CRP binding to the phosphocholine-modified screen-printed paper-based electrodes offers a low-cost method as it is an antibody-free specific binding platform. Our affinity-based PEID demonstrates great improvement in hs-CRP assays, offering the potential to evaluate the risk of future coronary events in individuals.

2. Materials and methods

2.1. Reagents and chemicals

All reagents and chemicals used in this experiment are described in the Supplementary material.

2.2. Design and fabrication of the PEID

The simple affinity folding PEID comprised a dual screen-printed working electrode and a counter-electrode coupled with a folding multilayer of wax-penetrated papers. To prepare the two-sided wax-based pattern on the 180 gsm office paper, the designed patterns of hydrophobic barriers as a dark blue-colour on a white background were fabricated using a slightly modified wax-printing procedure described in our previous study (Boonyasit et al., 2016a). Experimental details were described in Supplementary material. To assemble the whole system, the folding technique was used for fabrication of PEID, as illustrated in Fig. 1a. The designed wax-patterned paper electrochemical cell was composed of two paper working zones (2 mm in diameter) surrounded by shared counter electrodes. The wax patterns around the three electrodes constituted an insulator for the electrochemical cell and served as a reservoir with a volume of approximately 30 μL.

2.3. Surface modifications of PEID

The experiment was described in Supplementary material. An affinity-based impedance sensor was prepared by immobilising CDP-choline on the surface of the screen-printed paper-based electrodes via chitosan coating and glutaraldehyde cross-linking, as shown in Scheme S1.

2.4. Apparatus setup for the electrochemical impedance measurement

Details of apparatus setup for the electrochemical impedance measurement are in the Supplementary material. The configuration of the proposed system is illustrated in Fig. 1b.

3. Results and discussion

3.1. Surface characterisation of the folding affinity-based PEID

After the curing process, the wax-patterned A4 sheet was prepared for the screen-printing of the paper-based electrode configuration onto the hydrophilic zones. The procedure in details is included in the Supplementary material.

To investigate whether the surface of paper-based electrodes was successfully modified with chitosan, the fluorescence imaging experiment was also performed using the FITC staining technique. The FITC solution, an amine-reactive derivative of fluorescein dye, was prepared according to the manufacturer's instructions. Fig. 2a shows representative fluorescence micrographs of (1) a negative control without the modification of chitosan prepared in the same manner as the paper-based electrodes in the proposed PEID system and (2) a chitosan-modified paper-based electrodes stained with FITC. The results revealed that the paper-based electrodes were successfully modified with

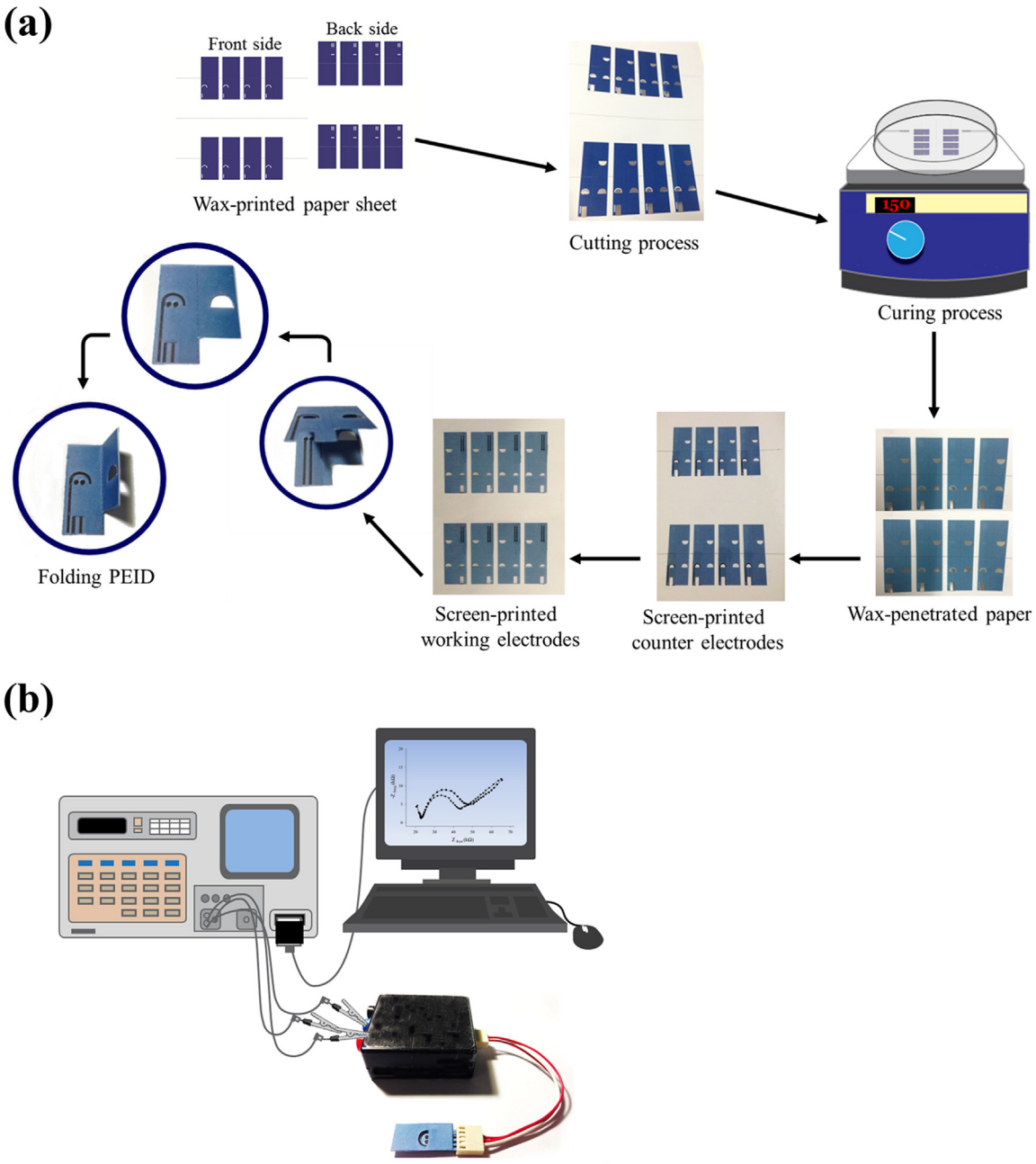

Fig. 1. Schematic representation of the proposed folding affinity-based PEID illustrating (a) the fabrication process for the paper-based electrodes and (b) the configuration of the label-free electrochemical impedance system set-up.

chitosan due to a binding interaction of isothiocyanate to primary amines present on the electrode surface. Additionally, the horseradish peroxidase-based enzyme linked immunoassay (HRP-based ELISA) application was also used for the detailed investigation of binding interactions of the phosphocholine-modified paper-based electrodes to CRP. To investigate whether the selective binding of phosphocholine residues and CRP molecules occurred on the surface of paper-based electrodes, the CRP-conjugated HRP antibody combined with the Amplex® UltraRed reagent, a fluorogenic substrate for HRP, was used for examining the presence of CRP on the sensing interfaces. Fig. 2b (Supplementary material) represents the fluorescence micrographs of (1) a negative control without CRP immobilisation and (2) CRP immobilisation on the electrode surface. The presence of fluorescence images implied that there was a specific binding of antigen-antibody complexes occurring on the electrode surface, indicating the successful immobilisation of CRP on the phosphocholine-modified paper-based electrodes.

3.2. Surface modifications and EIS characterisation

A dual screen-printed working paper electrode was subjected to step-wise modifications. The EIS measurements were carried out following each step of the surface modification at open circuit potential. Nyquist plots for the impedance measurements in the presence of 5 mM $[Fe(CN)_6]^{3-/4-}$ at different stages of the modification process are shown in Fig. 3a. Compared to the spectra obtained with the bare paper-based electrodes (curve 1), an increase in the Rct value was observed when the paper-based electrodes were modified with chitosan, which resulted from the blocking of the diffusion of the redox species to the electrode surfaces (curve 2). Subsequently, after modification of the chitosan-

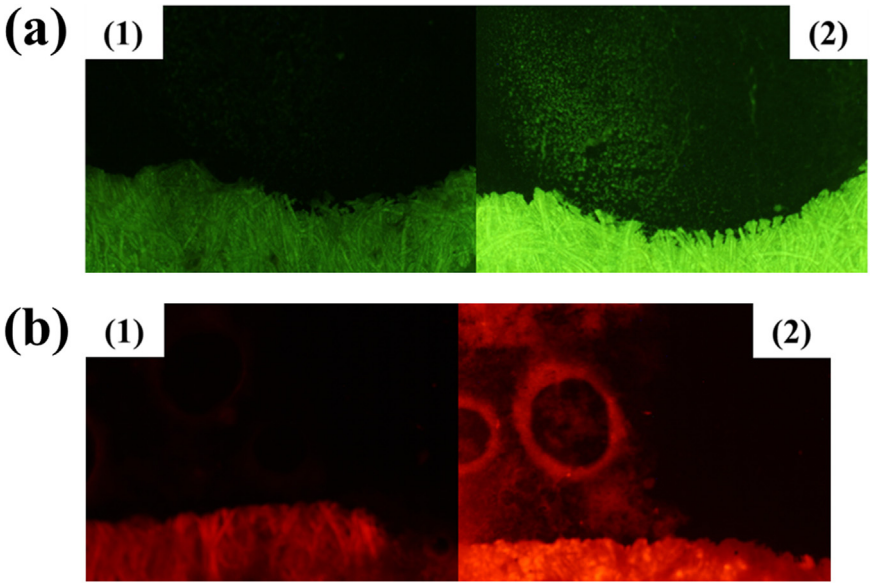

Fig. 2. Fluorescence micrographs of (a) FITC staining of the negative control without chitosan modification (1) and the positive control (2), and (b) Amplex® UltraRED staining of the negative control without CRP immobilisation (1) and the positive control (2).

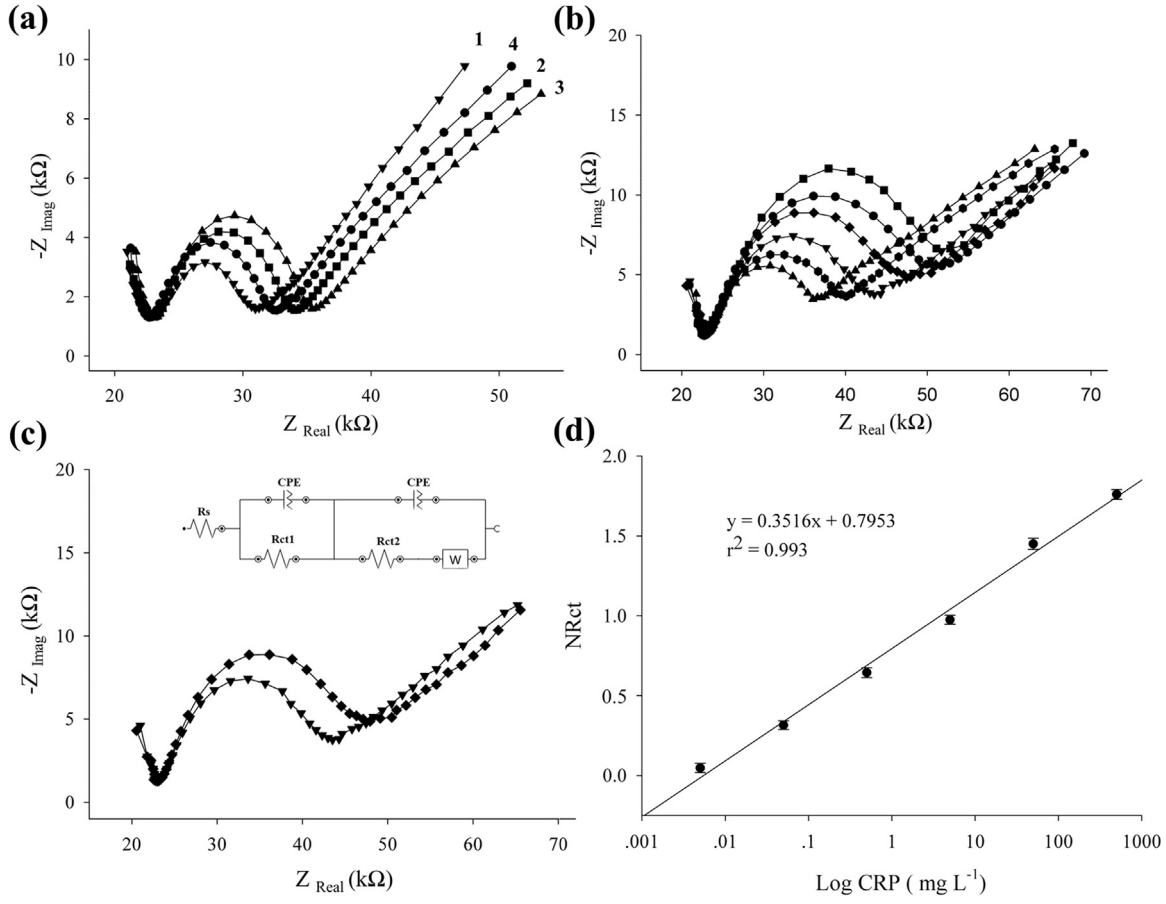

Fig. 3. Impedance data obtained from (a) the Nyquist plots for the stepwise analysis of the (▼) bare electrode, (■) chitosan-modified electrode, (▲) glutaraldehyde-treated electrode, and (•) phosphocholine-modified electrode; (b) the Nyquist plots of the phosphocholine-modified electrode after it was exposed to various concentrations of CRP: (▲) 0.005 mg L^{-1}, () 0.05 mg L^{-1}, (▼) 0.5 mg L^{-1}, () 5 mg L^{-1}, (•) 50 mg L^{-1}, and (■) 500 mg L^{-1}; (c) the Nyquist plots after incubation with (▼) 0.5 mg L^{-1}, and () 5 mg L^{-1} CRP standard solution. The solid lines represent curves fitted to the equivalent circuit in the inset. Inset: an equivalent circuit for analysing the impedance data; Rs, Rct, CPE, and W represent the solution resistance, charge-transfer resistance, constant-phase element, and Warburg impedance, respectively. The EIS spectra were obtained in 5 mM $Fe(CN)_6^{3-/4-}$ solution prepared in a working buffer at an open circuit voltage from 100 kHz to 10 MHz (ac amplitude, 10 mV); and (d) variation of the normalised Rct with respect to the concentration of CRP.

modified electrodes with the glutaraldehyde solution, a substantial increase in resistance was observed (curve 3). The glutaraldehyde-activated electrodes were further modified with CDP-choline before exposure to the various concentrations of CRP levels. The results showed that the impedance spectra obtained from the phosphocholine-modified electrodes were significantly lower than those from the glutaraldehyde-treated electrodes (curve 4). This indicates the increased electron transfer kinetics of the negatively charged $[Fe(CN)_6]^{3-/4-}$ redox couple due to the influence of the positive surface charge. However, the decrease in Rct after the immobilisation of CDP-choline cannot be fully explained since, instead, it causes repulsion of the redox probe. To investigate whether the surface features of the paper-based electrodes were successfully immobilised with CDP-choline, the control experiments were also performed using a dual paper-based electrode without immobilised CDP-choline prepared in the same manner as the proposed system. Because of the lack of any interaction between chitosan and CRP, the impedance signals remained unchanged compared to the baseline signals of the chitosan-modified electrodes, as shown in Fig. S2a. Additionally, the impedance signals of the glutaraldehyde-treated electrodes were not in direct proportion to the various concentrations of CRP, as shown in Fig. S2b, implying that the changes in impedance were due to the specific binding between the phosphocholine-modified electrodes and CRP.

3.3. Optimisation of the CRP assay

Some analytical parameters should be optimised, i.e., pH, chitosan and glutaraldehyde concentrations, and immobilisation time, before EIS measurements. Notably, the effect of pH has been widely perceived to be the most crucial factor for binding affinity. Therefore, in this study, the effect of pH on binding was investigated with a 0.1 M Tris-HCl buffer solution containing 150 mM KCl and 5 mM $CaCl_2$ to maintain the pH at 7, 8, or 9. As shown in Fig. S3 (Supplementary material), the normalised Rct values of the PEID system were higher at pH 8 than at pH 7. The results revealed that the sensitivity of the CRP assay increased with increasing pH. Although the binding complexes at pH 9 provided the highest sensitivity, it was disregarded due to the narrow linearity. Thus, pH 8 was used in all subsequent experiments, which is in agreement with previous findings (Kim et al., 2011, 2013b; Mackiewicz et al., 2010).

Different chitosan and glutaraldehyde concentrations were evaluated for sensor preparation using two clinically relevant levels of CRP (0.5 mg L^{-1} and 5 mg L^{-1}). As shown in Fig. S4a and S4b (Supplementary material), the Rct increased with increasing concentration until 0.5 mg mL^{-1} and 25%, respectively. These concentrations were, therefore, used in all subsequent experiments.

As the sensitivity for CRP recognition relies on the density of surface bound phosphocholine groups, different concentrations of CDP-choline were investigated. The Rct increased with increasing CDP-choline concentration, reaching a maximum at approximately 50 μg mL^{-1}, which indicates that the surface is becoming fully saturated with CDP-choline groups (Fig. S4c, Supplementary material). As a result, 50 μg mL^{-1} CDP-choline was used for preparation of the APBA modifications in all subsequent experiments.

As the number of functional groups and CRP molecules on the surface of the electrode affects the sensitivity of the sensor, the effect of immobilisation and incubation time on the determined Rct values was also studied. First, the time to immobilise 0.5 mg mL^{-1} chitosan and 50 μg mL^{-1} CDP-coline on a dual electrode surface was investigated for two different CRP concentrations (0.5 mg L^{-1} and 5 mg L^{-1}). Then, the incubation time of CRP was studied using a sensing surface prepared based on the optimised immobilisation time. The Rct increased steadily with the chitosan and CDP-choline immobilisation time from 5 to 30 min (Fig. S5a and S5b, Supplementary material), reaching a maximum after about 20 and 15 min, respectively, when assaying high and low CRP levels. This immobilisation time was used to prepare the sensing surfaces for further experiments. Similarly, the Rct increased with increasing CRP incubation time (Fig. S5c, Supplementary material), approaching a maximum after 10 min for both the high and low HbA1c level. Thus, a 10-min incubation time was determined to be the optimum condition and was used throughout the studies.

3.4. Analytical characteristics

Under optimal conditions, a remarkable increase in impedance values with increasing concentrations of CRP was observed in the Nyquist plot, as depicted in Fig. 3b. The binding interaction between the phosphocholine-modified electrodes and the CRP contents hindered the diffusion of redox species to the surface of paper-based electrode, thus making the redox process more difficult and causing the impedance to increase. Moreover, the dramatic changes in impedance were noticed at a lower frequency range, as shown in Fig. S6a, thereby demonstrating the sensitive response of the phosphocholine-modified electrodes towards CRP. The phase shift increased steadily upon the immobilisation of CRP and subsequent addition of higher CRP concentrations, as shown in Fig. S6b. To provide quantitative information on the effect of different electrode modifications and CRP concentrations, the acquired Nyquist plots were fitted to the modified Randles equivalent circuit model (Fig. 3c, inset), which includes a series of two constant-phase elements (CPEs) in parallel with two charge-transfer resistances (Rct) and the Warburg impedance (W), along with the resistance of the electrolyte solution (Rs). Ideally, Rs and W are not affected by modifications occurring at the electrode surface, whereas both Rct and CPE are altered by electrode modifications. Table S1 (Supplementary material) demonstrates the determined values of Rct, ZCPE (Q and α), and the effective equivalent capacitance (C_{eff}) derived from the ZCPE. Although the value of C_{eff} decreases as a consequence of successive modifications, the trend in C_{eff} is not clear when incubated with various CRP concentrations. The significant increases in Rct2 were observed with increasing CRP concentrations, thereby representing a great value for quantitative determination of CRP levels in blood samples. The solid lines in Fig. 3c show the fitting of Nyquist plots acquired after incubation with CRP standard solutions (0.5 mg L^{-1} and 5 mg L^{-1}), indicating that the equivalent circuit model describes the data well down to the lowest frequencies. According to the impedance values obtained from the fit to this equivalent circuit, an increase in the Rct was observed in the presence of increasing CRP concentrations. The normalised resistances derived from the fitted resistance values were plotted versus the various concentrations of CRP. As depicted in Fig. 3d, the substantial increases in impedance signal were directly proportional to CRP levels over the concentration range of 0.005 mg L^{-1} to 500 mg L^{-1}, with a regression equation of $y = 0.3516 \times + 0.7953$ ($r^2 = 0.993$) and a detection limit (3σ/slope) of 0.001 mg L^{-1}.

The correlation between the CRP concentration and each frequency was investigated to determine the optimal binding frequency at a specific binding constant. The relationship between the impedance signals derived from the phosphocholine-modified electrodes and CRP concentration was compared at each frequency point in the range from 100 kHz to 10 MHz and further analysed by reaching a compromise between the R-squared value and the correlation's slope, at which the maximised values were selected as the optimum binding target. The R-squared value and the slope from a duplicate measurement on a single paper-based electrode were plotted against the frequency range, as shown in Fig. 4a. The R-squared value increased from the baseline and reached a maximum value close to 1 before returning to a lower level, whereas the slope gradually decreased until reaching a value close to 0 as the frequency increased. Hence, the optimal frequency of the binding interaction between the phosphocholine-modified electrodes and CRP was determined to be 100 Hz. The correlation, as shown in Fig. 4b, represents an average impedance value of two different paper-based electrodes at a frequency of 100 Hz over a wide concentration gradient ranging from 0.005 mg L^{-1} to 500 mg L^{-1}, with a regression equation of

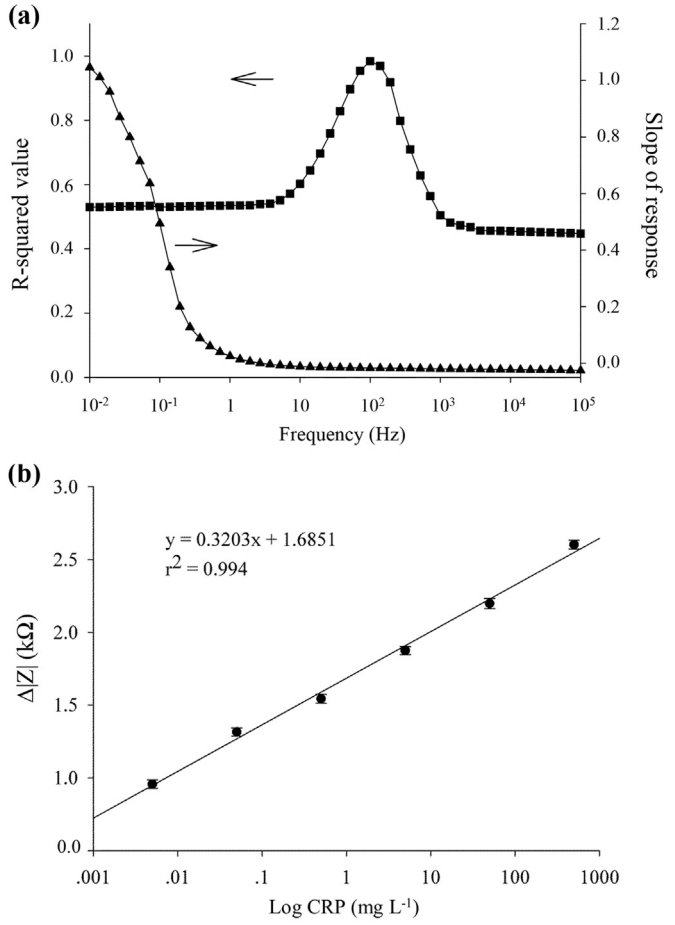

Fig. 4. Optimal binding frequency for (a) the phosphocholine-modified paper-based electrodes and CRP interaction: (■) R-squared value of response versus frequency, (▲) slope of response versus frequency; and (b) correlation between the average impedance response at a specific frequency and its associated CRP concentration.

$y = 0.3203 \times + 1.6851$ ($r^2 = 0.994$). We further investigated whether the standard curve obtained from an impedance measurement at a specific single-frequency could be used instead of that from an impedance measurement recording the entire frequency range. Within the 95% confidence interval, a paired statistical analysis showed no significant differences between the two methods (p-value = 0.001), indicating the potential benefit of using a single frequency value for analysis.

As demonstrated here, our PEID proposed for measuring cardiovascular risk markers not only improves the assay time by using a single specific-frequency measurement but also offers a great sensitivity to CRP values within the clinical requirement ranges. Our device is the first report on the detection of CRP based on an affinity-sensing device covering a broad clinical range. Table S2 in the Supplementary material provides a brief summary of the current EIS-based devices for assaying CRP. Thus, our proposed system provides a sensitive and cost-effective paper-based device for assessing cardiovascular risk in individuals.

3.5. Regeneration and reproducibility

The reversibility of the interactions between CRP and its specific recognition element was also investigated to assess the method's potential for diagnostic applications. To evaluate the performance of the regeneration procedure, the regeneration efficiency (RE) was calculated according to the previous studies (Boonyasit et al., 2016b; Yakovleva et al., 2002). Table S3 (Supplementary material) presents Rct data for the binding interaction on one electrode. In addition, 0.005 mg L^{-1} and 0.05 mg L^{-1} CRP caused an increase in Rct, similarly as shown in Fig. 3b. After regeneration using 0.1 M Tris-HCl containing 150 mM sodium chloride and 10 mM EDTA (pH 8), the Rct returned to the original value due to the release of CRP in both cases. The RE was 99.34% and 99.17% after the first and second regeneration cycle, respectively. After the second regeneration cycle, incubation with 0.005 mg L^{-1} CRP still caused a similar Rct increase, as was initially observed for that concentration. The results indicate that the interaction was reversible, facilitating the construction of a reusable CRP assay system. The reproducibility of our PEID was tested by determining both low (0.5 mg L^{-1}) and high (5 mg L^{-1}) CRP levels using a separate device for each concentration. Ten measurement cycles per device, each followed by a regeneration step, were run on each day for three consecutive days. Each measurement cycle comprised 2 acquired impedance spectra using a dual individually addressable measurement site on each device. The variation in measurements between individual electrodes, expressed as the relative standard deviation (RSD), was 2.82%. Considering the 10 measurement cycles per day for three days (n = 30), the overall assay reproducibility for each concentration, expressed as the relative standard error of mean (RSE%), was 1.21%. Moreover, the RSD for the CRP levels measured on ten independently fabricated paper-based sheets was 2.11%, offering an acceptable reproducibility of fabrication. These results indicate that our proposed system provides a great precision for the detection of CRP with an acceptable reproducibility of fabrication.

The stability of the PEID system was investigated over a period of 7 days. The immobilised PEIDs were kept under dry conditions in a vacuum desiccator cabinet until assay. To evaluate the activity of the individual paper-based electrodes, the impedance response was determined every day using 5 mg L^{-1} CRP standard solution. Fig. S7 (Supplementary material) shows that the activity of the phosphocholine sensing interface was 91.14% over a four-day period; however, after 7 days, the signal response had retained 80% of its initial response to CRP. The decrease in signal was probably caused by the loss of binding activity during the prolonged storage period. Long-term storage stability of the device should be further investigated.

3.6. Selectivity study

The evaluation of endogenous and exogenous interfering substances present in clinical specimens is essential before the diagnostic system can be implemented clinically. Thus, to assess the analytical performance of the proposed system for measuring cardiovascular risk markers, human serum albumin, fibrinogen, and immunoglobulin G were tested as potential interferences in the sensing interfaces. In this study, a known quantity of each interfering substance was spiked into the 0.5 mg L^{-1} CRP standard solutions, and the recovery percentage was assessed to determine how much the spiked signal increased or decreased from the initial response signals. Table S4 (Supplementary material) shows that 8000 mg dL^{-1} of human serum albumin impacted the CRP assays, resulting in the recovery of 122.6%. However, the measured recoveries dropped to satisfactory levels of 102.8% and 99.8% when the amount of human serum albumin was decreased to 6000 mg dL^{-1} and 3000 mg dL^{-1}, respectively. Moreover, a fibrinogen concentration of 600 mg dL^{-1} and 100 mg dL^{-1} generated reasonable recovery signals of 105.1% and 101.2%, respectively. Similarly, the effect of immunoglobulin G covering a concentration range of 600–1800 mg dL^{-1} was acceptable with recoveries between 100.0% and 104.7%. These results indicate that the proposed PEID system was highly selective in determining the CRP values in actual specimens, enabling the possibility of using the present method to assess the cardiovascular risk in individuals.

3.7. Real sample analysis and assay comparison

A demonstration of the ability of the diagnostic system to detect the

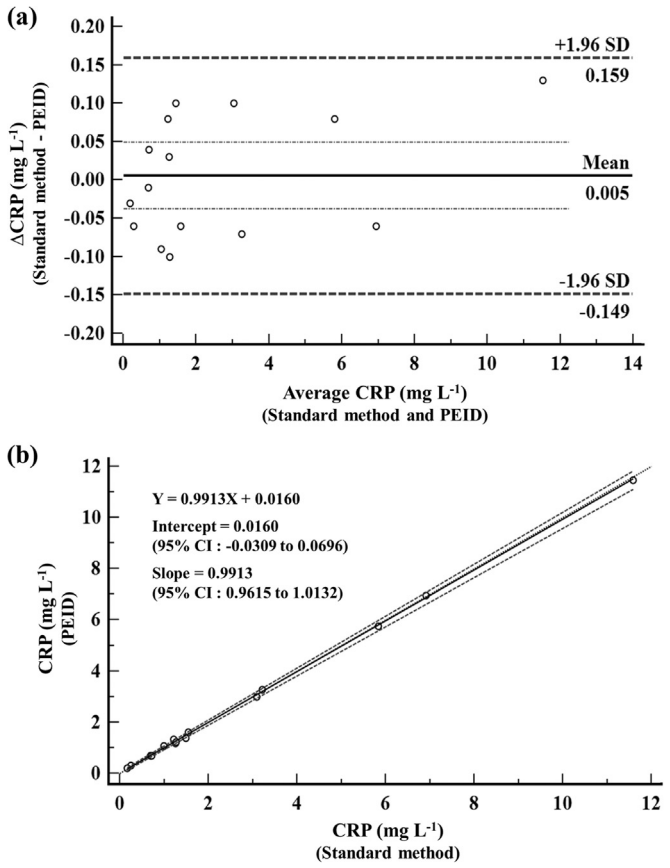

Fig. 5. Comparison of the proposed folding affinity-based PEID and the current large-scale method for CRP measurements using (a) a Bland-Altman bias plot and (b) Passing-Bablok regression analysis, respectively.

hs-CRP in real human blood samples is essential before it can be implemented clinically. Thus, to further investigate its potential practical application, the effectiveness of the proposed PEID for measuring CRP values was assessed using the real blood samples of healthy, diabetic, and hypertensive volunteers. Each plasma sample was measured individually using our system and with the automated clinical chemistry analyser. The results obtained from the proposed PEID were compared with those determined with the particle-enhanced immunoturbidimetric assay on an automated large-scale analyser. The agreement and correlation between the two approaches were evaluated via a Bland-Altman bias plot and a Passing-Bablok regression analysis, respectively. As demonstrated in Fig. 5A, the data showed acceptable agreement between the results provided by our proposed device and the commercially available kit within an agreement interval of ± 1.96 SD. These results also showed zero bias and a reliable relationship, which indicates that these two approaches could be used interchangeably. Moreover, as shown in Fig. 5B, the regression equations according to the Passing-Bablok analysis of the CRP was y = 0.9913 × + 0.0160. These results indicated a good correlation between the two methods throughout the entire measurement range. Within a 95% confidence interval, the values of the y-intercept (0.0160 mg L^{-1}) and the slope (0.9913) were significantly reliable and covered a range from -0.0309–0.0696 mg L^{-1} and 0.9615–1.0132, respectively. The data presented in this proof-of-concept work demonstrates the validity of the proposed device for the ultrasensitive detection of hs-CRP in clinical diagnostics using actual clinical specimens. Our paper-based devices offer the great benefit of an onsite clinical test for assessment of future cardiovascular risk in healthy individuals.

4. Conclusions

The proposed affinity-based PEID not only provides an ultrasensitive measurement of hs-CRP that covers the clinically relevant ranges, but also offers a wide dynamic concentration range for assaying CRP. This ultrasensitivity was obtained because of the simple folding of the PEID forming a small electrochemical chamber. Antibody-free EIS sensing on a paper electrode makes this cost-effective device useful for assessing cardiovascular risk in healthy individuals. The system performed well compared with the commercial automated method using actual clinical samples. By monitoring at a single frequency value, the proposed device has a considerable advantage over the conventional EIS measurements in terms of assay time, allowing a decrease in the data acquisition time.

Acknowledgements

This research was financially supported by the Thailand Research Fund through Research Team Promotion Grant (RTA6080002). Y.B. acknowledges the support from the Rachadapisek Sompot Fund for Postdoctoral Fellowship, Chulalongkorn University.

Appendix A. Supplementary material

Supplementary data associated with this article can be found in the online version at doi:10.1016/j.bios.2018.09.031.

References

Ahn, J.S., Choi, S., Jang, S.H., Chang, H.J., Kim, J.H., Nahm, K.B., Oh, S.W., Choi, E.Y., 2003. Clin. Chim. Acta 332 (1), 51–59.
Ala-Kleme, T., Mäkinen, P., Ylinen, T., Väre, L., Kulmala, S., Ihalainen, P., Peltonen, J., 2006. Anal. Chem. 78 (1), 82–88.
Bhattacharyya, A., Klapperich, C., 2007. Biomed. Micro. 9 (2), 245–251.
Boonyasit, Y., Chailapakul, O., Laiwattanapaisal, W., 2016a. Anal. Chim. Acta 936, 1–11.
Boonyasit, Y., Heiskanen, A., Chailapakul, O., Laiwattanapaisal, W., 2015. Anal. Bioanal. Chem. 407 (18), 5287–5297.
Boonyasit, Y., Laiwattanapaisal, W., Chailapakul, O., Emnéus, J., Heiskanen, A.R., 2016b. Anal. Chem. 88 (19), 9582–9589.
Borque, L., Bellod, L., Rus, A., Seco, M.L., Galisteo-González, F., 2000. Clin. Chem. 46 (11), 1839–1842.
Bryan, T., Luo, X., Bueno, P.R., Davis, J.J., 2013. Biosens. Bioelectron. 39 (1), 94–98.
Centi, S., Bonel Sanmartin, L., Tombelli, S., Palchetti, I., Mascini, M., 2009. Electroanalysis 21 (11), 1309–1315.
Christodoulides, N., Tran, M., Floriano, P.N., Rodriguez, M., Goodey, A., Ali, M., Neikirk, D., McDevitt, J.T., 2002. Anal. Chem. 74 (13), 3030–3036.
de Ávila, B.E.-F., Escamilla-Gómez, V., Campuzano, S., Pedrero, M., Salvador, J.-P., Marco, M.-P., Pingarrón, J.M., 2013. Sens. Actuators, B 188, 212–220.
Deegan, O., Walshe, K., Kavanagh, K., Doyle, S., 2003. Anal. Biochem. 312 (2), 175–181.
Dupuy, A.M., Badiou, S., Descomps, B., Cristol, J.P., 2003. Clin. Chem. Lab. Med. 41 (7), 948–949.
Elshafey, R., Tavares, A.C., Siaj, M., Zourob, M., 2013. Biosens. Bioelectron. 50, 143–149.
Fairchild, A.B., McAferty, K., Demirok, U.K., LaBelle, J., 2009. ICME International Conference on Complex Medical Engineering, 1-5.
Fernandes, F.C., Santos, A., Martins, D.C., Goes, M.S., Bueno, P.R., 2014. Biosens. Bioelectron. 57, 96–102.
Gan, N., Wang, L., Zhou, H., Li, T., Sang, W., Hu, F., Cao, Y., 2012. Int. J. Electrochem. Sci. 7, 11564–11577.
Gan, N., Xiong, P., Wang, J., Li, T., Hu, F., Cao, Y., Zheng, L., 2013. J. Anal. Methods Chem. 2013.
Goda, T., Toya, M., Matsumoto, A., Miyahara, Y., 2015. ACS Appl. Mater. Interfaces 7 (49), 27440–27448.
Hennessey, H., Afara, N., Omanovic, S., Padjen, A.L., 2009. Anal. Chim. Acta 643 (1), 45–53.
Hu, W.-P., Hsu, H.-Y., Chiou, A., Tseng, K., Lin, H.-Y., Chang, G.-L., Chen, S.-J., 2006. Biosens. Bioelectron. 21 (8), 1631–1637.
Islam, M.S., Lee, H.G., Choo, J., Song, J.M., Kang, S.H., 2010. Talanta 81 (4), 1402–1408.
Katz, E., Alfonta, L., Willner, I., 2001. Sens. Actuators, B 76 (1), 134–141.
Kazimierczak, B., Pijanowska, D., Baraniecka, A., Dawgul, M., Kruk, J., Torbicz, W., 2016. Biocybern. Biomed. Eng. 36 (1), 29–41.
Kiernan, U.A., Addobbati, R., Nedelkov, D., Nelson, R.W., 2006. J. Proteome Res. 5 (7), 1682–1687.
Kim, C.-H., Ahn, J.-H., Kim, J.-Y., Choi, J.-M., Lim, K.-C., Park, T.J., Heo, N.S., Lee, H.G., Kim, J.-W., Choi, Y.-K., 2013a. Biosens. Bioelectron. 41, 322–327.
Kim, B.B., Im, W.J., Byun, J.Y., Kim, H.M., Kim, M.-G., Shin, Y.-B., 2014. Sens. Actuators, B 190, 243–248.
Kim, E., Kim, H.-C., Lee, S.G., Lee, S.J., Go, T.-J., Baek, C.S., Jeong, S.W., 2011. Chem.

Commun. 47 (43), 11900–11902.
Kim, E., Lee, S.G., Kim, H.-C., Lee, S.J., Baek, C.S., Choi, E.-S., Jeong, S.W., 2013b. Sep. Sci. Technol. 48 (17), 2600–2607.
Kitayama, Y., Takeuchi, T., 2014. Anal. Chem. 86 (11), 5587–5594.
Kokkinos, C., Prodromidis, M., Economou, A., Petrou, P., Kakabakos, S., 2015. Anal. Chim. Acta 886, 29–36.
Koukouvinos, G., Petrou, P., Misiakos, K., Drygiannakis, D., Raptis, I., Stefanitsis, G., Martini, S., Nikita, D., Goustouridis, D., Moser, I., 2016. Biosens. Bioelectron. 84, 89–96.
Kriz, K., Ibraimi, F., Lu, M., Hansson, L.-O., Kriz, D., 2005. Anal. Chem. 77 (18), 5920–5924.
Kumar, D., Prasad, B.B., 2012. Sens. Actuators, B 171, 1141–1150.
La Belle, J.T., Demirok, U.K., Patel, D.R., Cook, C.B., 2011. Analyst 136 (7), 1496–1501.
Lasseter, T.L., Cai, W., Hamers, R.J., 2004. Analyst 129 (1), 3–8.
Lehr, J., Fernandes, Fv.C.B., Bueno, P.R., Davis, J.J., 2014. Anal. Chem. 86 (5), 2559–2564.
Libby, P., Ridker, P.M., 2004. Am. J. Med. 116 (6), 9–16.
Mackiewicz, M.R., Hodges, H.L., Reed, S.M., 2010. J. Phys. Chem. B 114 (16), 5556–5562.
McBride, J.D., Cooper, M.A., 2008. J. Nanobiotechnology 6 (1), 1.
Meyer, M.H., Hartmann, M., Keusgen, M., 2006. Biosens. Bioelectron. 21 (10), 1987–1990.
Meyer, M.H., Hartmann, M., Krause, H.-J., Blankenstein, G., Mueller-Chorus, B., Oster, J., Miethe, P., Keusgen, M., 2007. Biosens. Bioelectron. 22 (6), 973–979.
Meyer, K., Ueland, P.M., 2014. Anal. Chem. 86 (12), 5807–5814.
Miao, W., Bard, A.J., 2003. Anal. Chem. 75 (21), 5825–5834.
Mitsakakis, K., Gizeli, E., 2011. Anal. Chim. Acta 699 (1), 1–5.
Noble, J., Attree, S., Horgan, A., Knight, A., Kumarswami, N., Porter, R., Worsley, G., 2012. Anal. Chem. 84 (19), 8246–8252.
O'Reilly, E.J., Conroy, P.J., Hearty, S., Keyes, T.E., O'Kennedy, R., Forster, R.J., Dennany, L., 2015. RSC Adv. 5 (83), 67874–67877.
Oh, S.W., Moon, J.D., Park, S.Y., Jang, H.J., Kim, J.H., Nahm, K.B., Choi, E.Y., 2005. Clin. Chim. Acta 356 (1), 172–177.
Park, H.E., Cho, G.-Y., Chun, E.-J., Choi, S.-I., Lee, S.-P., Kim, H.-K., Youn, T.-J., Kim, Y.-J., Choi, D.-J., Sohn, D.-W., 2012. Atherosclerosis 224 (1), 201–207.
Park, J.-Y., Lee, Y.-S., Kim, B.H., Park, S.-M., 2008. Anal. Chem. 80 (13), 4986–4993.
Peoples, M.C., Karnes, H.T., 2008. Anal. Chem. 80 (10), 3853–3858.
Periyakaruppan, A., Gandhiraman, R.P., Meyyappan, M., Koehne, J.E., 2013. Anal. Chem. 85 (8), 3858–3863.
Phurimsak, C., Tarn, M.D., Pamme, N., 2016. Micromachines 7 (5), 77.
Phurimsak, C., Tarn, M.D., Peyman, S.A., Greenman, J., Pamme, N., 2014. Anal. Chem. 86 (21), 10552–10559.
Pomowski, A., Baricham, C., Rapp, B.E., Matern, A., Länge, K., 2015. IEEE Sens. J. 15 (8), 4388–4392.
Prasad, S., Selvam, A.P., Reddy, R.K., Love, A., 2013. J. Lab. Autom. 18 (2), 143–151.
Pultar, J., Sauer, U., Domnanich, P., Preininger, C., 2009. Biosens. Bioelectron. 24 (5), 1456–1461.
Raj, V., Hari, P., Sreenivasan, K., 2007. Anal. Chim. Acta 592 (1), 45–50.
Ridker, P.M., 2003. Circulation 107 (3), 363–369.
Rifai, N., Ridker, P.M., 2001. Clin. Chem. 47 (1), 28–30.
Roberts, W.L., 2004. Circulation 110 (25), e572–e576.
Sadir, S., Prabhakaran, M.P., Wicaksono, D.H., Ramakrishna, S., 2014. Sens. Actuators, B 205, 50–60.
Senju, O., Takagi, Y., Uzawa, R., Iwasaki, Y., Suzuki, T., Gomi, K., Ishii, T., 1986. J. Clin. Lab. Immunol. 19 (2), 99–103.
Shervedani, R.K., Hatefi-Mehrjardi, A., 2007. Sens. Actuators, B 126 (2), 415–423.
Shervedani, R.K., Mozaffari, S.A., 2006. Anal. Chim. Acta 562 (2), 223–228.
Singal, S., Kotnala, R.K., 2017. Appl. Biochem. Biotechnol. 1–12.
Songjaroen, T., Feeny, R.M., Mensack, M.M., Laiwattanapaisal, W., Henry, C.S., 2016. Sens. Biosensing Res. 8, 14–19.
Thomas, N.E., Coakley, W.T., 1996. Ultrasound Med. Biol. 22 (9), 1277–1284.
Vashist, S.K., Czilwik, G., van Oordt, T., von Stetten, F., Zengerle, R., Schneider, E.M., Luong, J.H., 2014. Anal. Biochem. 456, 32–37.
Vattipalli, K., Feikert, P., Brandigampala, S., Prasad, S., 2010. Nano Life 175–183.
Vermeeren, V., Grieten, L., Bon, N.V., Bijnens, N., Wenmackers, S., Janssens, S., Haenen, K., Wagner, P., Michiels, L., 2011. Sens. Actuators, B 157 (1), 130–138.
Wu, T.-L., Tsai, I.C., Chang, P.-Y., Tsao, K.-C., Sun, C.-F., Wu, L.L., Wu, J.T., 2007. Clin. Chim. Acta 376 (1), 72–76.
Yakovleva, J., Davidsson, R., Lobanova, A., Bengtsson, M., Eremin, S., Laurell, T., Emnéus, J., 2002. Anal. Chem. 74 (13), 2994–3004.
Yang, Y.-N., Lin, H.-I., Wang, J.-H., Shiesh, S.-C., Lee, G.-B., 2009. Biosens. Bioelectron. 24 (10), 3091–3096.
Zhou, F., Lu, M., Wang, W., Bian, Z.-P., Zhang, J.-R., Zhu, J.-J., 2010. Clin. Chem. 56 (11), 1701–1707.
Zhou, G., Mao, X., Juncker, D., 2012. Anal. Chem. 84 (18), 7736–7743.